Bulletin of the Seismological Society of America, Vol. 93, No. 1, pp. 152–171, February 2003

Field Test of an Inexpensive, Small Broadband Ocean-Bottom Seismograph

by Jay Pulliam, Yosio Nakamura, Carlos Huerta-Lopez,* and Ben Yates

Abstract We conducted tests of a three-component broadband ocean-bottom seismograph (OBS), including side-by-side comparisons with the broadband Global Seismic Network/U.S. National Seismic Network station HKT at Hockley, Texas, and a 28-day deployment in the Gulf of Mexico. Our goals were to evaluate seismometer performance and determine whether our seafloor deployment strategy allows useful earthquake data to be collected. The seismometer generally performed well, but showed unexpectedly high intrinsic noise at frequencies above 1 Hz and produced occasional spikes that were confined to a single component at a given time. We identified 32 earthquakes from the Gulf of Mexico data; only five additional events were observed at the nearby, highly sensitive station HKT on land. While noise levels were higher throughout the 0.01–20 Hz frequency band in the Gulf of Mexico compared with HKT, site amplification effects in the gulf were only significant at frequencies above 1 Hz and power in most earthquake signals peaked at frequencies below 0.1 Hz, nearly coinciding with a minimum in background noise. We found the seismometer and OBS package encouraging for far-regional and teleseismic studies, given the low cost of the OBS and inexpensive means for deployment and recovery, but less encouraging for detecting and locating small-magnitude local and near-regional events.

Introduction

There are important differences between seafloor and continental regimes with respect to earthquake seismology. Background noise on the ocean floor tends to be higher than on continents, and the shape of the noise spectrum is skewed—with a microseismic peak at higher frequencies than on continents and a noise trough below 0.1 Hz (see Webb [1998] for a thorough review). Second, researchers seeking to deploy instruments face special challenges, given the difficulty in accessing remote and deep seafloor sites and the poorly consolidated, water-saturated sediments that cover the majority of the ocean basins. Technology for emplacing seismographs in boreholes well below the seafloor and burying them shallowly in sediments is being developed and tested (Collins *et al.*, 2001; Duennebier, 1997) and will make critical contributions to broadband seismology in the oceans. Recent tests have demonstrated an impressive capacity of shallow burial to reduce background noise levels on seismographs (Collins *et al.*, 2001). However, while they tend to be less demanding than emplacing a seismograph in a subseafloor borehole, strategies demonstrated for shallow burial so far are still more time consuming, more expensive, and more cumbersome than typical methods of deployment and recovery of short-period ocean-bottom seismographs (OBSs). An inexpensive broadband OBS that is deployed with a simple and fast "drop" strategy would hold significant cost and logistical advantages over burial strategies which, given the vast expanse of ocean floor to be canvassed and the great cost of operations at sea, would allow more instruments to be built, deployed, and recovered for available, fixed funding. We tested such a seismograph and deployment strategy in order to determine whether data useful for targeted studies of the deep Earth, from earthquakes located at regional and teleseismic distances, could be recorded and whether PMD Scientific Inc.'s innovative seismometer is a suitable candidate for the seismograph. To this end, we modified a University of Texas Institute for Geophysics (UTIG) OBS to incorporate a PMD 2123 seismometer and conducted a series of tests on land, in an inland lake in Texas, and in the Gulf of Mexico. The PMD 2123 seismometer utilizes molecular electronic transducers instead of the traditional pendulum-based design, which results in an inexpensive, small, lightweight, and rugged seismometer with low power requirements that is highly tolerant of tilt.

There is great interest among the marine science community in broadband OBSs (BBOBSs) with the capabilities outlined above, as is indicated by the broad workshop participation that culminated in the report "Broadband Seismology in the Oceans" (Purdy, 1995) domestically, and

*Present address: Departamento de Sismología, Centro de Investigación Científica y de Educación Superior de Ensenada (CICESE), Km 107 Carretera Tijuana-Ensenada, Ensenada, 22860, B.C. México.

among the Japanese (e.g., Suyehiro, 1997), French (Montagner *et al.*, 1994), and Russians (Dozorov and Soloviev, 1991) internationally. More recently, a large and diverse group of investigators collaborated to collect earthquake data with OBSs at the Southern East Pacific Rise for the mantle electromagnetic and tomography (MELT) experiment (Forsyth *et al.*, 1998a). The MELT experiment successfully demonstrated the capability of relatively narrowband instruments deployed on the seafloor to record for periods on the order of 6 months. Other successful OBS recordings of teleseisms were summarized by Blackman *et al.* (1995).

UTIG's Broadband Ocean-Bottom Seismograph

UTIG's OBS consists of a 14-bit analog-to-digital convertor (ADC) with gain-ranging, that is, the amplifier's gain is dynamically adjusted by software to utilize the full range of the ADC yet avoid clipping of large-amplitude signals. The ADC is thus equivalent to 21 bits with a maximum of 10 V peak to peak. A fourth-order Butterworth (low-pass) antialias filter is set by plug-in resistor blocks and can be changed to fit the requirements of each deployment. The internal temperature compensated crystal oscillator (TXCO) clock is accurate to 2 parts in 10^{-7} and tends to drift quite linearly at the nearly constant temperature on the seafloor. Calibrations conducted before and after deployment with a Global Positioning System clock allow corrections to be made that result in accuracy of 1 part in 10^{-8}. Data are stored in a 512 kB memory buffer and then written to a magnetic disk drive. The device is powered by a series of battery cells that, along with the OBS's three-component sensor and data acquisition system, are all packaged inside a 43-cm glass sphere. The glass sphere, which is certified to withstand pressures equivalent to a water depth of 6.8 km, is attached to a steel frame anchor by means of an elastic cord fastened with a burn wire. The OBS is deployed by simply dropping it overboard at the desired location, following programming and clock calibration. After the OBS reaches bottom and begins operating (at a preset time), the ship steams across the OBS twice in a crossing pattern while shooting a small air gun. Water wave arrivals are later used to determine the OBS's precise location and the orientation of its horizontal components (Nakamura *et al.*, 1987). At the conclusion of an experiment an acoustic signal is sent to the OBS that triggers an electric current through the burn wire. In salt water this current causes the wire to separate, freeing the OBS from its anchor, whereupon it floats to the surface and flashes a strobe light and radio beacon to aid in recovery.

Because all functional elements of the OBS are enclosed in the same sphere, noise produced by the spinning magnetic disk interferes with the acquisition of seismic data from the seismometer. This interference means that short time gaps in data acquisition are introduced as data stored in memory are written to the disk. The frequency of data gaps depends on the size of the memory buffer and the sample interval. We recorded 40 samples/sec in our tests, which resulted in data gaps of roughly 22 sec every 36 min. These data gaps are a significant annoyance that could hinder data analysis, but new technology will render them relatively unimportant, in our view, and will be among the innovations introduced with a new data acquisition package, as discussed below.

An OBS intended for earthquake studies must incorporate a seismometer that has a broad passband, is small and light in weight, has low power requirements, is rugged, and is relatively insensitive to out-of-plane orientation, whether through its own design or due to gimbaling. PMD Scientific's seismometers have received a great deal of attention from seismologists recently and have been found to perform well in separate tests (e.g., Urhammer, 1997). The PMD 2123 seismometer we tested is 17.8 cm in diameter by 11.8 cm high, weighs 4.5 kg, and has nominal sensitivity of 1500 V/(m/sec). Rather than the traditional pendulum-based design, the PMD 2123 utilizes a molecular electronic transducer, which has no moving mechanical parts (Abramovich *et al.*, 1997). Our seismometer's response, throughout the tests reported here, was flat to velocity from 0.033 to 50 Hz (Fig. 1), which includes sensitivity to periods below the microseism ("noise") peak and includes most of the "noise notch," a band of frequencies for which background noise is relatively low in the oceans (Webb, 1998). The PMD 2123 does not incorporate a force-balance feedback mechanism, so nonlinearity in response might be a concern for deployments in which strong motions are to be recorded. Abramovich *et al.* (2001) described recent nonlinearity tests and PMD's plans to address this issue. During the tests at Hockley and the Gulf of Mexico, discussed here, the seismometer drew 15 mA current at 12 V, for total power consumption of 180 mW. Our seismometer has since been modified by PMD Scientific to draw 5 mA at 12 V, for total power consumption of 60 mW, and to have a passband flat to velocity from 0.0167 to 20 Hz.

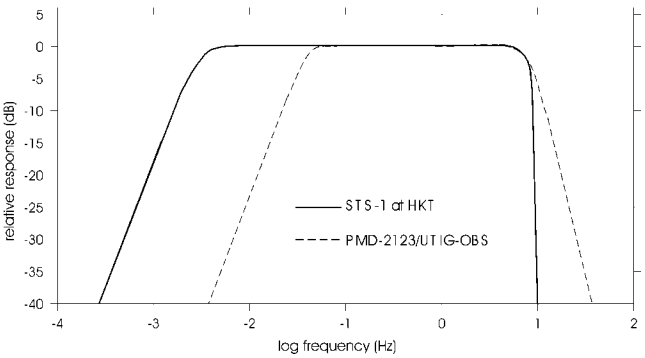

Figure 1. Passbands of PMD 2123 and Streckeisen STS-1 seismometers. Data from the PMD 2123 were recorded by the UTIG OBS data acquisition system, which consists of a gain-ranged 14-bit ADC, for nominal dynamic range equivalent to 21 bits. This combination is referred in this paper as BBOBS. See text for details about the UTIG OBS package. The STS-1, digitized by a 24-bit Quanterra Q680 and recorded by IRIS's GSN, is referred to here as HKT.

Table 1
Earthquakes Recorded during Instrument Tests

Date (yyyy/mm/dd)	Origin Time	Latitude (°)	Longitude (°)	Depth (km)	Magnitude	Location
Recorded at Hockley, Texas						
1999/4/5	11:08:04.0	5.591S	149.568E	150.0	7.3 M_L	New Britain Region, P.N.G.
Recorded in the Gulf of Mexico						
1999/07/16	13:45:25.5	23.775 N	108.708 W	10.0	5.1 M_b	Gulf of California
1999/07/19	02:17:03.6	28.629 S	177.608 W	39.0	6.3 M_b	Kermadec Islands Region
1999/07/19	17:56:33.6	15.654 N	88.317 W	10.0	4.8 M_L	Honduras
1999/07/21	13:46:29.7	4.567 N	97.211 E	175.0	5.9 M_b	Northern Sumatra, Indonesia
1999/07/26	01:33:20.2	5.151 S	151.942 E	69.0	6.1 M_L	New Britain Region, P.N.G.
1999/07/27	23:30:20.0	15.201 S	173.324 W	33.0	5.4 M_b	Tonga Islands
1999/07/28	00:16:57.5	28.690 S	177.523 W	33.0	6.0 M_L	Kermadec Islands Region
1999/07/28	10:08:20.6	30.285 S	178.014 W	25.0	6.1 M_b	Kermadec Islands, New Zealand
1999/07/29	21:50:42.2	17.024 N	94.252 W	135.0	5.0 M_b	Chiapas, Mexico
1999/07/31	07:11:35.2	5.201 N	82.579 W	10.0	4.8 M_b	South of Panama
1999/08/01	08:39:04.9	30.367 S	177.832 W	10.0	6.4 M_s	Kermadec Islands, New Zealand
1999/08/01	12:47:50.1	51.520 N	176.273 W	33.0	5.8 M_L	Andreanof Islands, Aleutian Islands
1999/08/01	16:06:22.0	37.390 N	117.080 W	8.0	5.7 M_b	California–Nevada Border Region
1999/08/01	20:10:54.3	52.303 N	173.381 W	51.0	5.2 M_b	Andreanof Islands, Aleutian Islands
1999/08/02	01:06:37.7	33.023 S	70.153 W	95.0	5.2 M_b	Chile–Argentina Border Region
1999/08/02	06:05:13.0	37.380 N	117.070 W	3.0	5.1 M_b	California–Nevada Border Region
1999/08/03	15:58:57.6	3.453 S	79.162 W	88.0	5.9 M_L	Near Coast of Ecuador
1999/08/04	16:49:50.7	31.656 S	68.079 W	115.0	5.4 M_b	San Juan Province, Argentina
1999/08/05	04:35:49.3	12.234 N	86.614 W	10.0	5.0 M_L	Nicaragua
1999/08/05	04:50:55.1	12.563 N	86.717 W	10.0	4.5 M_b	Nicaragua
1999/08/05	05:31:48.2	12.612 N	86.544 W	10.0	5.0 M_b	Nicaragua
1999/08/05	07:11:15.7	12.343 N	86.724 W	10.0	5.1 M_L	Nicaragua
1999/08/05	08:01:51.4	12.605 N	86.728 W	10.0	4.4 M_b	Nicaragua
1999/08/05	09:20:28.8	12.525 N	86.649 W	10.0	5.0 M_L	Nicaragua
1999/08/06	00:32:41.7	49.933 N	156.261 E	58.0	5.8 M_L	Kuril Islands
1999/08/06	18:53:18.0	12.606 N	86.660 W	10.0	4.9 M_b	Nicaragua
1999/08/07	06:17:28.8	21.086 S	176.059 W	33.0	5.3 M_s	Fiji Islands Region
1999/08/07	07:42:45.9	12.140 N	86.553 W	10.0	4.5 M_b	Nicaragua
1999/08/09	12:57:59.0	1.804 N	85.380 W	10.0	4.3 M_b	Off Coast of Ecuador
1999/08/09	22:58:45.3	51.229 N	178.062 E	33.0	5.4 M_b	Rat Islands, Aleutian Islands
1999/08/10	14:55:42.4	9.346 N	83.967 W	33.0	5.2 M_L	Costa Rica
1999/08/12	05:44:59.5	1.716 S	122.456 E	33.0	6.1 M_L	Sulawesi, Indonesia

Figure 1 compares the passband of the PMD 2123 with that of the Streckeisen STS-1 installed in the permanent station HKT at Hockley, Texas, a member of the Global Seismic Network (GSN) of the Incorporated Research Institutes for Seismology (IRIS) and the U.S. National Seismic Network (USNSN) of the U.S. Geological Survey (USGS). HKT is located 478 m below ground in a working salt mine and, despite occasional blasts related to mining activities, has extremely quiet noise characteristics in the frequency band of interest for earthquake recordings. Furthermore, the STS-1 seismometer installed at HKT is highly sensitive and has extremely low intrinsic noise, in addition to its broad passband, and is operated with a true 24-bit Quanterra Q680 digitizer. We did not expect the broadband OBS to rival HKT's high standard, but the comparison is useful as a benchmark in side-by-side tests and for an investigation of seafloor conditions and properties when the OBS is deployed offshore in the Gulf of Mexico. In this article we will refer to the Streckeisen seismometer and Quanterra digitizer combination simply as "HKT" and to the PMD 2123 seismometer and UTIG data acquisition package as "BBOBS."

Results of a Side-by-Side Comparison

BBOBS and HKT records of an event in Papua New Guinea (5 April 1999; Table 1) are shown in Figure 2. Essential features are consistent between the seismographs' records, although the BBOBS data (bottom) show greater high-frequency noise than do the HKT data (top). While fairly large in magnitude, this event occurred at an epicentral distance of 114°, so both *P* and *S* arrivals are diffracted. Body-wave portions of the records are compared in detail in Figure 3, where arrivals on the BBOBS (solid lines) match HKT arrivals (dashed lines) quite well in terms of timing, but tend to underestimate the larger amplitude excursions. The reason for the discrepancy in higher frequency noise content between the two seismographs is revealed by an examination of coherence between components of the BBOBS and HKT seismographs (Fig. 4) and from respective power spectral density (PSD) estimates (Fig. 5). Coherence between respective components, computed for the time interval shown in Figure 2, rises from below 0.5 at 0.01 Hz to roughly 0.75 at the low corner frequency of the PMD 2123, is nearly unity

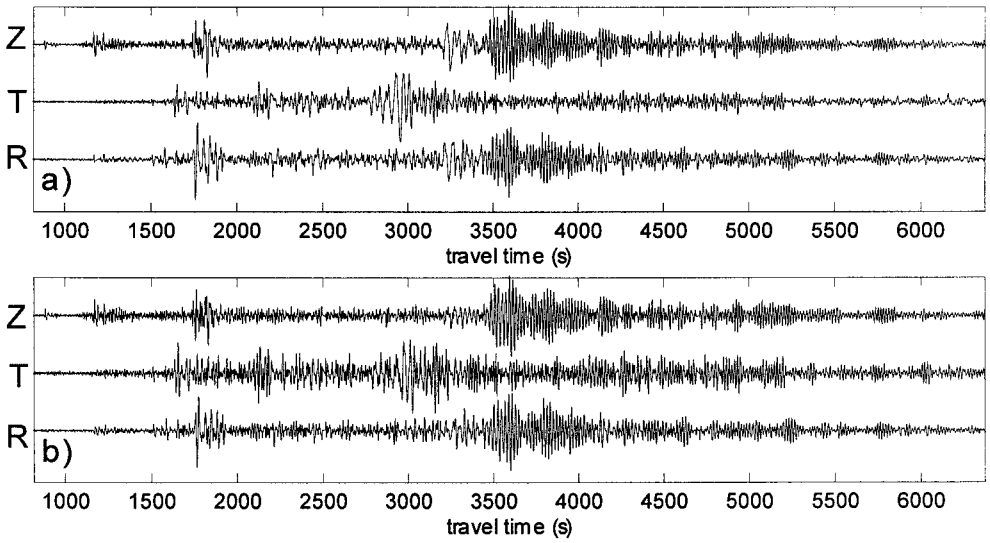

Figure 2. Rotated and trace-normalized records of the 5 April 1999 Papua New Guinea earthquake (Table 1) recorded by (a) station HKT and (b) the BBOBS. Both instruments were located on the same concrete pier at Hockley, Texas, at a distance of 114° from the earthquake. A fifth-order butterworth bandpass filter with corner frequencies at 0.01 and 5 Hz was applied to records from both seismographs.

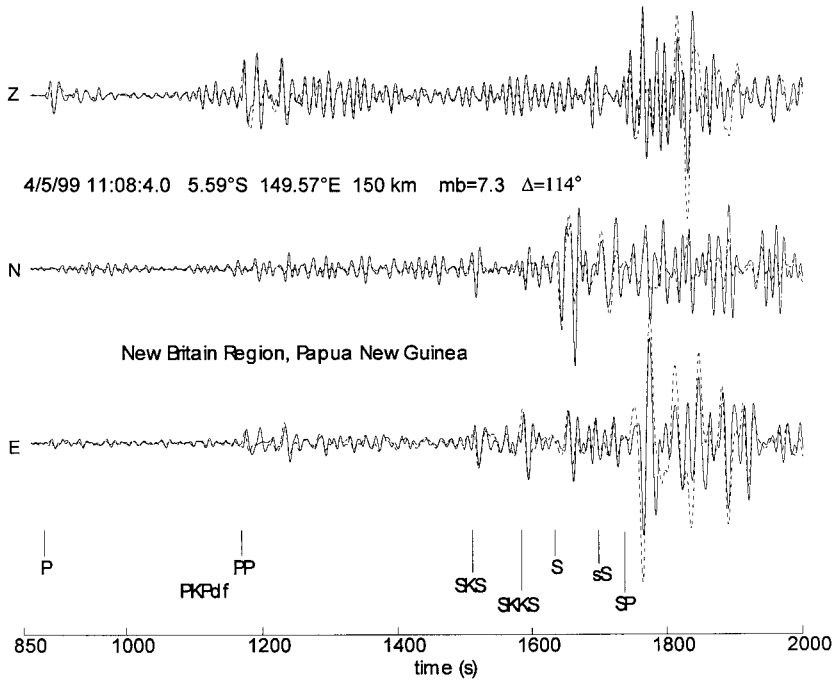

Figure 3. Detailed comparison between BBOBS data (solid lines) and HKT data (dashed lines) for the 5 April 1999 Papua New Guinea earthquake. Raw velocity data have been filtered with corner frequencies at 0.01 and 1 Hz, windowed about body-wave phases, and normalized to the maximum amplitude on each trace.

between 0.05 and 1 Hz, and drops off rapidly above 1 Hz for the horizontal components and above 2.5 Hz for the vertical components. PSD estimates, shown in Figures 5 and 6, suggest the reason for poor coherence at higher frequencies: the PMD 2123 has a much higher noise floor than the STS-1 at frequencies above 1 Hz.

PSD estimates were obtained using time series subsegments of 4096 points each, with an overlap of 75%. The mean value of each subsegment was removed, and a Hanning window of 4096 points was applied to each subsegment. The averaged PSD estimates were then normalized with respect to the subsegment length, the frequency increment Δf of the obtained PSD, and amplitude scaling due to the symmetry property of the discrete Fourier transform, which is periodic with period N, where N is the subsegment number of points. After correcting for the instrument response, spectral amplitudes were transformed in the frequency domain to units of acceleration. BBOBS time series

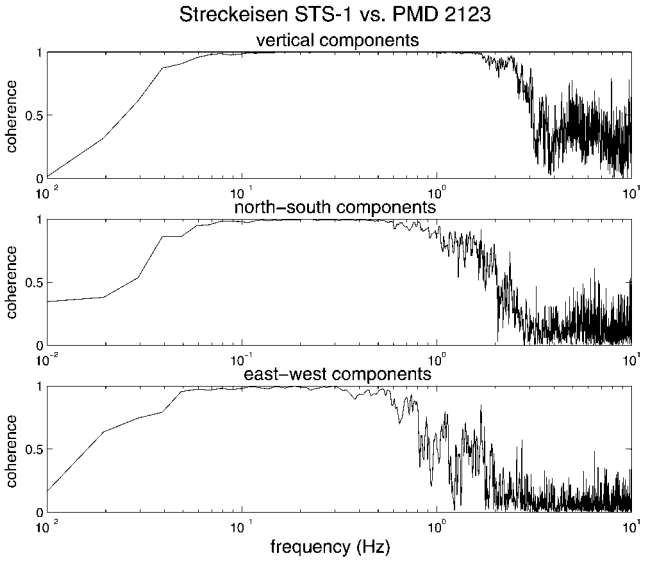

Figure 4. Coherence between respective components of HKT and BBOBS for the time window of Figure 2. The lack of coherence above about 1 Hz is due to the high noise floor above 1 Hz on the BBOBS and the lack of significant power above that noise floor in the teleseismic signals.

were tapered at the beginning and end of each data gap. Figure 5a and b shows the PSD estimates for the 5 April 1999 Papua New Guinea earthquake from the BBOBS and HKT, respectively. Note the similarity between PSDs for comparable components for frequencies up to 1 Hz, then the dissimilarity at higher frequencies. Figure 5c and d shows PSD estimates for background noise immediately preceding the earthquake's arrival on 5 April 1999. Figure 5c also shows the digitization noise of the UTIG OBS data acquisition system, recorded with a resistor in place of the seismometer during a later test in our lab. This figure indicates that digitization noise during normal operation is not the source of the high noise floor above 1 Hz. Gain-ranging—switching the value of the least significant count during the arrival of a large signal—is not the cause either. A close examination of the BBOBS data revealed that the gain level did not change during the recording of this event.

Figure 6 compares PSDs for background noise and the earthquake signals shown in Figure 2 for the three components of each seismograph. Energy peaks at 0.05–0.06 Hz for this teleseismic event, at nearly the same frequency at which the PMD 2123 reaches a local minimum. The BBOBS noise PSD rises rapidly from there, due to the rolloff of the instrument's passband, so the poor coherence at the low-frequency portion of the spectrum should be expected. Similarly, the high noise floor on the BBOBS above 1 Hz, relative to HKT, suggests that the two time series will be incoherent. This clearly is cause for concern, particularly for applications on land and for recording local earthquakes, but the low-noise "notch" that characterizes broadband noise spectra in the oceans (Dozorov and Soloviev, 1991; Webb, 1998) and the frequency content of teleseismic and regional earthquake signals make the PMD 2123 well suited for marine use. It would be helpful to compare signals for a local event or explosion that contains coherent energy above 1 Hz, but the Hockley region is relatively aseismic and we did not record a local event.

Results of Deployment in the Gulf of Mexico

The site chosen for a test deployment is approximately 150 nautical miles ESE of Port Aransas, Texas, in the Gulf of Mexico (Fig. 7). This site was chosen because it is flat over a fairly broad area, has sedimentary evidence of recent structural activity likely to have been caused by tectonically active salt domes (Satterfield and Behrens, 1990), is near a teleseismically determined earthquake epicenter (Frohlich, 1982), and is deep enough that the instrument was unlikely to be caught in a fishing net. The BBOBS was deployed on 15 July 1999 and came to rest on the seafloor at 1478 m below sea level. Recording continued uninterrupted for 4 weeks until 12 August 1999 on three channels at a sample rate of 40 samples/sec. Shortly after deployment and immediately before recovery, we shot two short crossing seismic lines over the instrument using a 60-in.^{3} (1 L) air gun in order to locate and determine the orientation of the instrument on the seafloor. Figure 8 shows the BBOBS just before deployment.

To analyze the data we simulated 24-hr drum records for the BBOBS and HKT seismographs and scanned both sets visually for earthquakes. The most eventful 24-hr period, shown in Figure 9, illustrates most features of the recordings, including a swarm of shallow events in Nicaragua (Table 1), as well as noise from several sources. First, several isolated noise spikes appear on the horizontal components (Fig. 9b and c), at roughly 14:45 on the horizontal 1 (Fig. 9b) and 19:33 on the horizontal 2 (Fig. 9c), for example, but do not appear on either of the other components at the same times. In general, we observed larger amplitude spikes more frequently during tests on land than in water, leading us to wonder whether the spiking is related to heat. Because it is sealed, the BBOBS does not dissipate heat well, particularly in a hot environment. The March/April 1999 BBOBS recordings at HKT, which is located 478 m below ground and is consistently about 100°F (38°C), contained many more spikes than did the Gulf of Mexico records. We also observed frequent spikes in several other summer tests in Texas, during which temperatures peaked above 100°F each day. In contrast, a test in Junction, Texas, during January and February 2000 produced relatively few spikes compared with the March/April 1999 Hockley test. Huerta-Lopez *et al.* (2002) described efforts to identify sources of background noise during our Gulf of Mexico deployment in a companion paper.

We identified 32 earthquakes of various sizes and epicentral distances (Table 1; Fig. 10) during the 4-week deployment. Figure 11 plots earthquake magnitude versus epi-

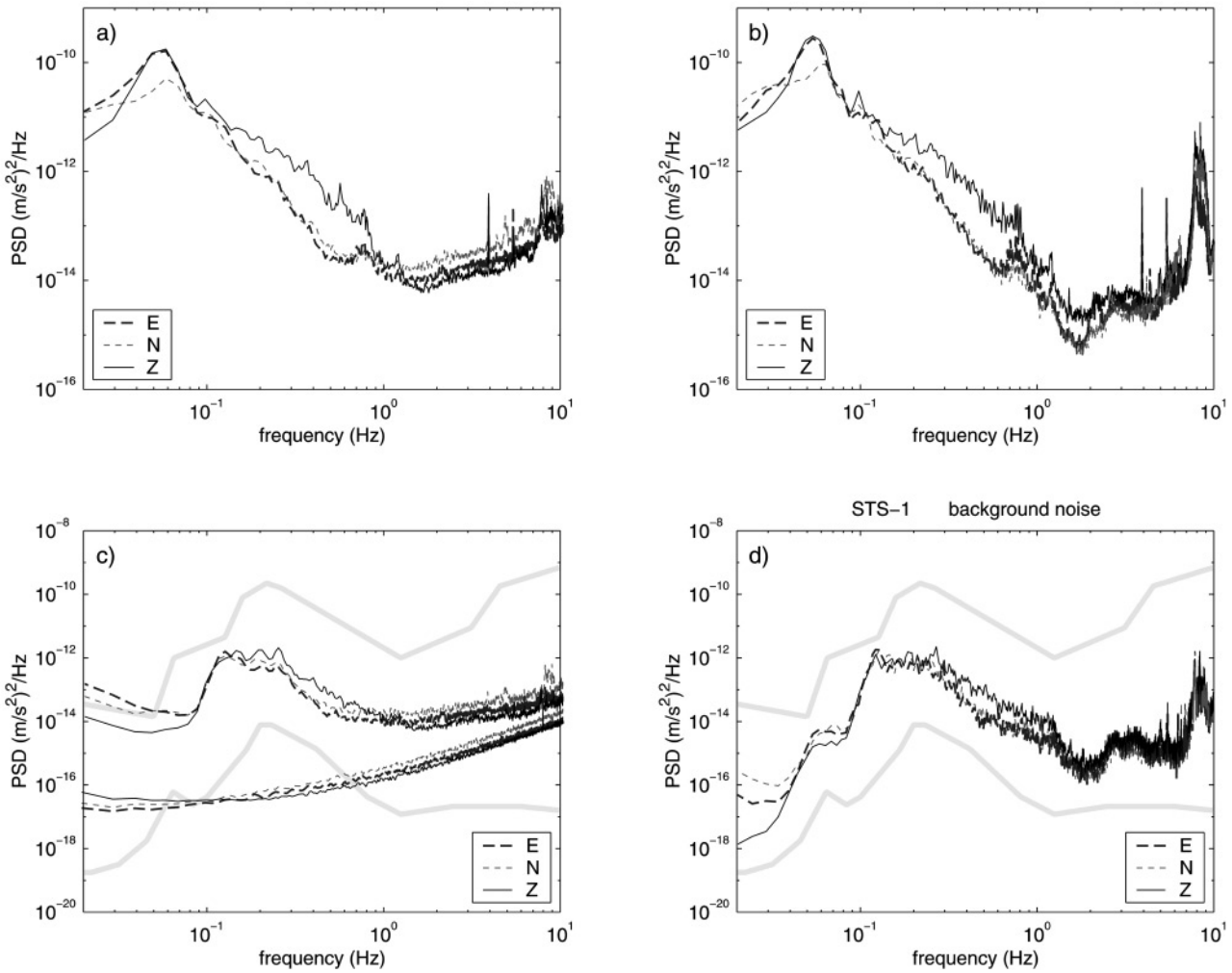

Figure 5. PSD estimates for the 5 April 1999 Papua New Guinea earthquake (Table 1) recordings made by (a) BBOBS and (b) HKT for the time window of Figure 2. All data were corrected for the instrument response. See text for further details of the PSD processing. PSDs of the 36 min of background noise preceding the first arrivals from the earthquake were also computed and are shown for (c) the BBOBS and (d) HKT. The most significant differences between the BBOBS and HKT are at frequencies less than 0.033 Hz (the corner frequency for the PMD 2123 at the time) and above 1 Hz, where the BBOBS noise floor is much higher than that of HKT. Digitization noise, as recorded separately in our lab, is superimposed on panel (c) (lower lines) and shows that the higher noise level above 1 Hz is not due to the UTIG OBS digitizer. The thick lines in panels (c) and (d) are the USGS low- and high-noise models compiled by Peterson (1993).

central distance to reveal a rough "detection threshold" for comparison with the highly sensitive, well-situated station HKT. On a three-tiered scale of phase-pick quality, 25 of the 32 events' *P* arrivals rated an "A," meaning they were impulsive and highly useful for locating the events; 5 rated "B," meaning they were more emergent; 1 rated a "C," meaning it was highly emergent; and 1 was unrated since it arrived during a data gap. Fifteen *S* arrivals rated "A"; 5 rated a "B," and 12 rated "C." An additional five events were detected at HKT that were not detected in the BBOBS data from the gulf. These were all relatively small events at epicentral distance between 15° and 42°. The vast majority of events, of course, were small and distant and not detectable on either seismograph. In a companion paper to this one, Huerta-Lopez *et al.* (2002) concluded that the background noise recorded by the BBOBS was associated with wind speed (including a time lag) and strongly correlated with wave height in the vicinity of the deployment site, as recorded by three permanently moored weather buoys operated by the National Oceanic and Atmospheric Administration (NOAA) (Fig. 7). Wilcock *et al.* (1999) compared OBS noise characteristics at sites on the East Pacific Rise and Iceland and concluded that an observed disparity in *P*-wave arrival detection between the sites is due to noise differences at about 1 Hz and that noise at 1 Hz is

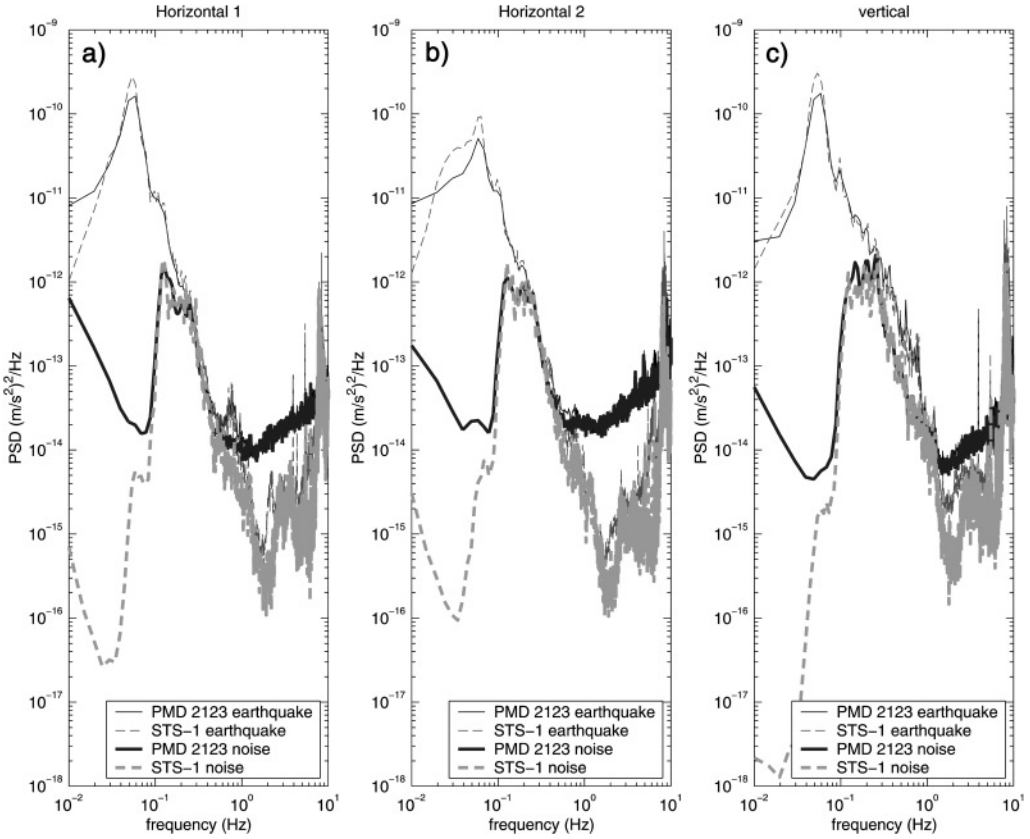

Figure 6. Comparison between HKT and BBOBS (a) east-west, (b) north-south, and (c) vertical component PSD estimates for background noise (thick lines) and the 5 April 1999 earthquake (thin lines). Note that teleseismic event reaches its peak power at about 0.05 Hz, whereas the peak power in the background noise is at 0.1–0.2 Hz.

controlled primarily by wind speed above the sites. Of the five events detected at HKT but not by our BBOBS, three occurred during the periods of highest wind speed, one during a moderate period, and one during a period of low wind speed. Due to the strong correlation between BBOBS background noise and wind speed and wave heights, it appears that bottom currents interacting with the BBOBS were minor contributors to background noise during our Gulf of Mexico experiment. As a result, we are unable to address Duennebier and Sutton's (1995) conclusion, from a burial test off Oahu in 1990, that "burial of sensor packages below the ocean floor can greatly decrease noise problems caused by currents."

Records from both HKT and the BBOBS of an event that occurred on 19 July 1999 in the Kermadec Islands are shown in Figure 12. Note the much greater high-frequency noise on the BBOBS, compared with HKT, the leaking of compressional energy onto the horizontal components, and the signal-generated noise following body-wave arrivals on the BBOBS. Figure 13 shows an enlarged view of body-wave seismograms from the 19 July 1999 Kermadec Islands event, filtered to a 0.01–0.5 Hz frequency band. Note that much of the high-frequency energy has been removed from the BBOBS records, which now appear similar in character to the HKT records. Also, energy correlated with the arrivals of compressional waves has disappeared from the BBOBS horizontal components and the shear-wave energy that dominates the horizontal components is largely absent from the BBOBS vertical component. The appearance of compressional energy on the horizontal components is most likely caused by high-frequency energy scattered near the BBOBS site, since the energy on the horizontal components that corresponds to compressional wave arrivals is strongly concentrated in higher frequencies. The signal-generated noise may be explained by scattering also, as well as by amplification of shear modes in the soft sedimentary layers, as determined through modeling of horizontal-to-vertical spectral ratios by Huerta-Lopez *et al.* (2002). Tilt induced by the bottom currents could also cause cross talk between components, in which case shear energy would appear on the vertical component. However, evidence of such cross talk would appear in the form of coherence between horizontal and vertical components, but for the time windows shown in Figure 13 and for the preceding 36 min of background noise, coherence does not exceed 0.25 for frequencies less than 2.5 Hz. This suggests that instrument tilt is not a major source of noise.

If scattering and amplification predominantly account for the cross-coupling between components and signal-gen-

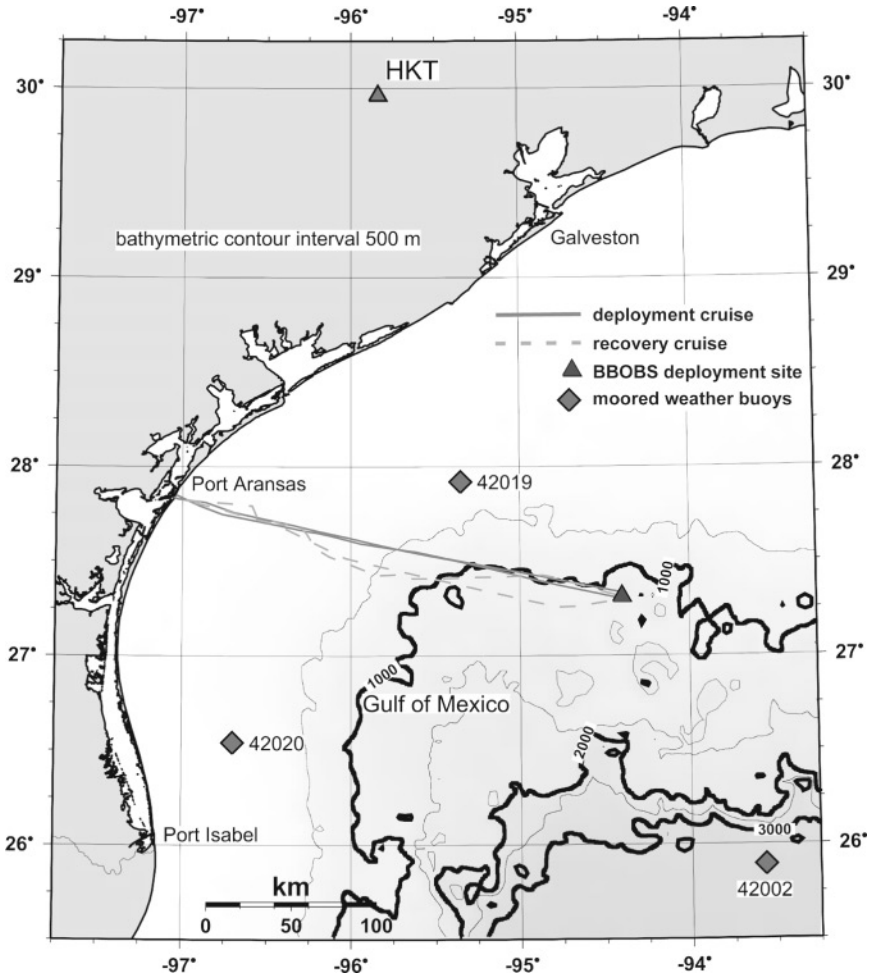

Figure 7. Map of Gulf of Mexico deployment site (27°18.36′N, 94°23.49′E), showing the routes to and from the deployment site (triangle) taken by the deployment and recovery cruises, the locations of the three closest NOAA weather buoys (diamonds), and the permanent GSN/USNSN station HKT. Water depth at the site was 1478 m.

Figure 8. Photograph of BBOBS prior to deployment in the Gulf of Mexico. The 17-inch glass sphere, in which the BBOBS's data acquisition package, sensor, and batteries are enclosed, may be deployed to water depths of 6 km.

erated noise, then neither would decrease substantially if the seismometer were buried in sediments a few meters below the seafloor. To reduce these sources of noise the seismometer would have to be installed beneath the soft sediment layers, more than 50 m beneath the seafloor. Bradley *et al.* (1997) reported that significant noise reduction with increasing depth is limited to frequencies above 0.5 Hz, although Duennebier and Sutton (1995) and Collins *et al.* (2001) presented theory and data, respectively, that show noise reduction at frequencies below 1 Hz as well.

However, another potential explanation is ringing due to imperfect coupling between the BBOBS and the seafloor. Trehu (1985) demonstrated that OBS–sediment coupling can be modeled as a mass-spring-dashpot system in which the resonant frequency and damping are determined by the instrument mass and bearing radius and shear modulus of the shallow sediments. Results of an *in situ* comparison between four different anchor types in the frequency range 2–60 Hz showed clear peaks in amplitude spectra between 3 and 6 Hz for a silty bottom and between 6 and 15 Hz for a sandy

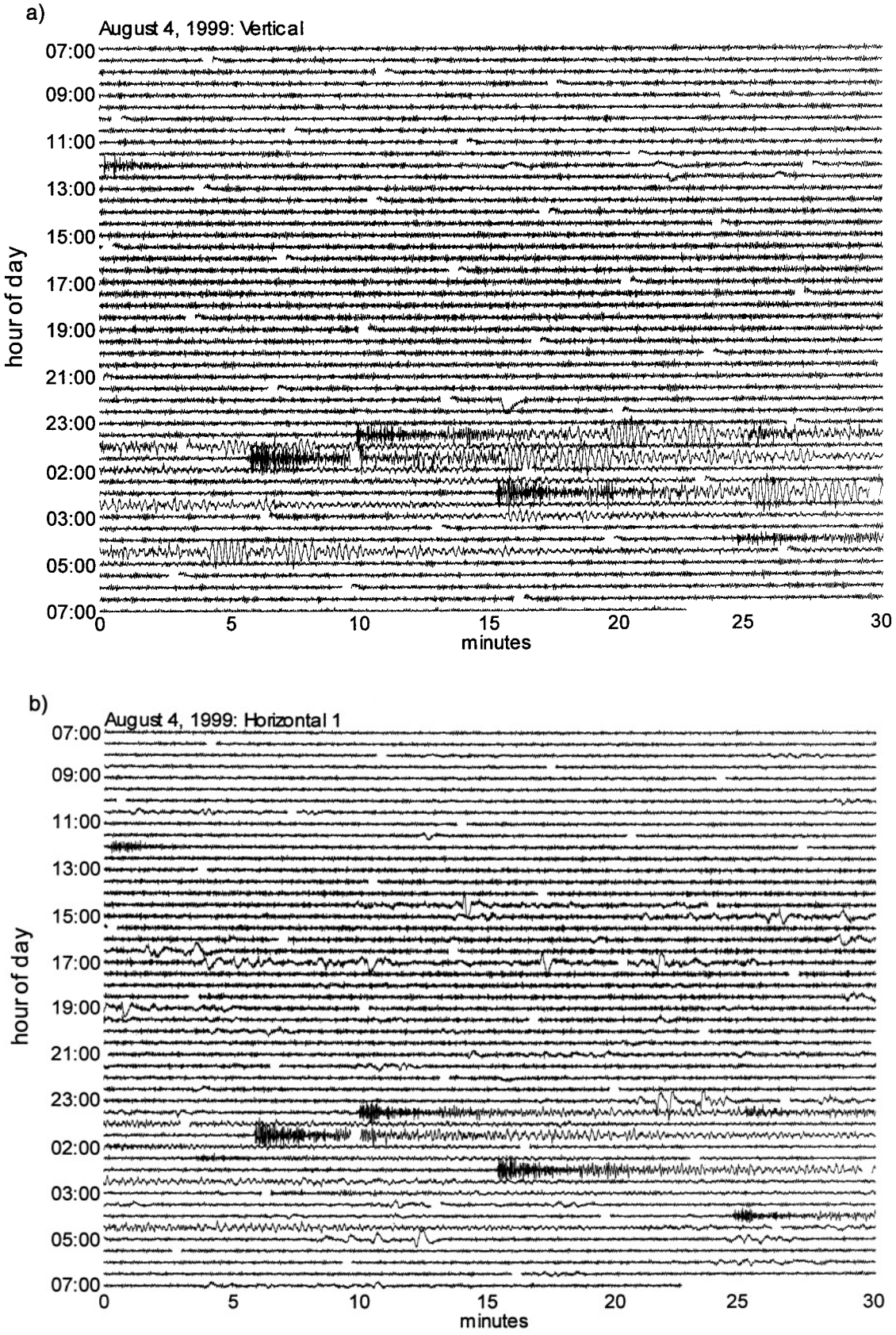

Figure 9. *Caption on following page.*

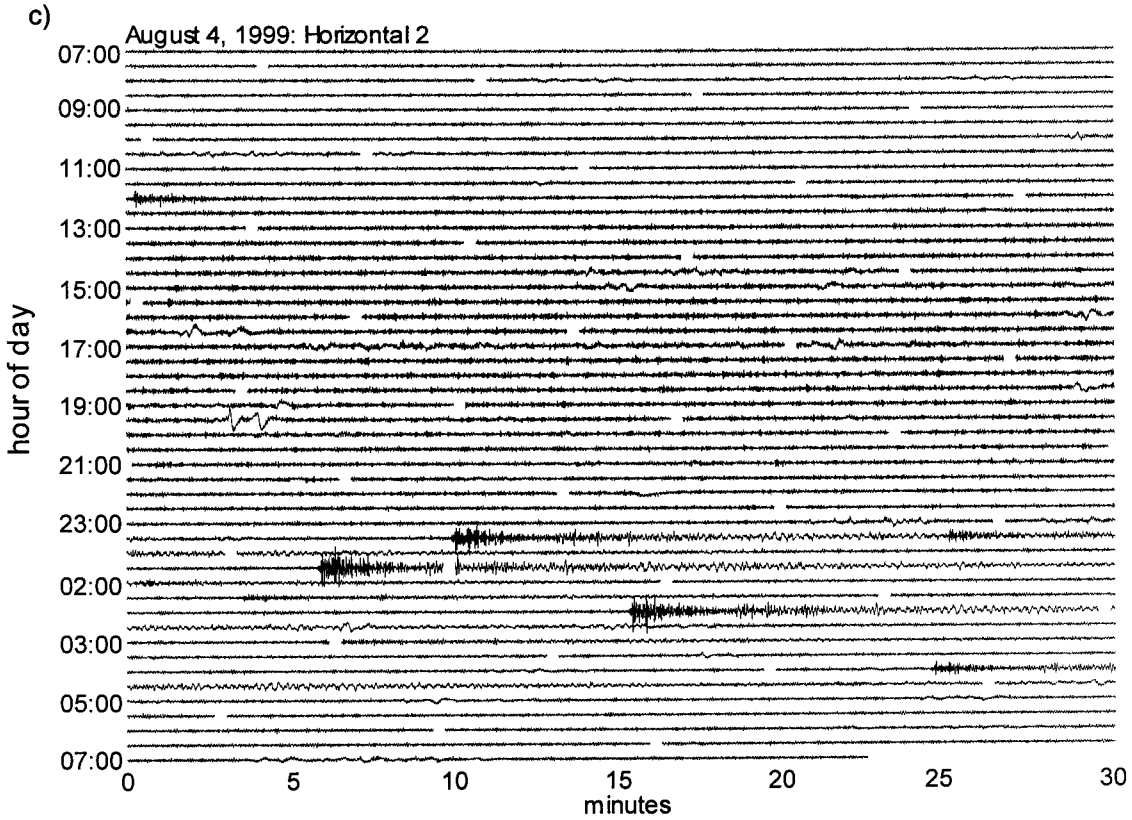

Figure 9. Raw digital output of the BBOBS (PMD 2123) (a) vertical component, (b) horizontal 1 component (azimuth 42.8°), and (c) horizontal 2 component (azimuth 132.8°) deployed in the Gulf of Mexico on 4 and 5 August 1999, plotted as a simulated 24-h drum record.

bottom; the experiments were repeatable in the same locations with highly consistent results. Anchor geometry appeared to strongly influence coupling characteristics for the vertical component, but only weakly, if at all, for the horizontal components. Trehu's (1985) preferred perforated plate anchor served to move the resonance to higher frequencies for both bottom types and for both vertical and horizontal components. Of the four types studied, our anchor is most similar to the perforated plate in size, weight, and open design. Coupling characteristics could therefore explain why the signal-generated noise is concentrated in frequencies above 1 Hz. If so, improved coupling, which might be accomplished by either shallow burial or borehole installation, might reduce this source of noise. However, if coupling resonances are limited to frequencies above 2 Hz, as indicated by Trehu (1985), it is unlikely that such installation will generally improve conditions in the 0.03–0.1 Hz low-noise notch, where teleseismic energy is concentrated.

Figure 14 shows PSD estimates for both earthquake and noise records, similar to those shown in Figure 5. Note the much greater noise levels on the BBOBS across the entire frequency band compared with the same time period at HKT (Fig. 14b and d). The relatively large power levels on the BBOBS horizontal components between 0.7 and 2 Hz are due to shear modes amplified by the soft shallow sediments (Huerta-Lopez *et al.*, 2002). Energy from the 19 July 1999 Kermadec Islands event, located at a distance of 97.18° from the BBOBS, is concentrated in frequencies below 0.2 Hz and peaks at about 0.06 Hz (Fig. 15), so the amplification effect of the BBOBS site at higher frequencies is of little consequence for such teleseisms. Figure 15 illustrates the fortunate coincidence of the teleseismic energy peak's correlation with a trough in background noise succinctly. For each component, BBOBS power for the time window of Figure 12 is plotted along with BBOBS power for the 36-min interval immediately preceding the earthquake. HKT power is plotted for the same time intervals; both sets of curves indicate relatively little power from the earthquake above 0.2 Hz.

Figure 16a and b shows additional, moderate-sized Kermadec Islands events, bandpass filtered as in Figure 13. At this distance the core-penetrating *SKS* and *SKKS* phases, which are polarized in the radial direction due to conversions from compressional to shear waves upon reentering the mantle from the core, arrive just before the direct *S* phase. All three arrivals appear clearly on both sets of records. The minimax *SS* phase, which reflects off of the Earth's surface roughly midway between the source and receiver, appears prominently in Figure 16a and less prominently in Figure

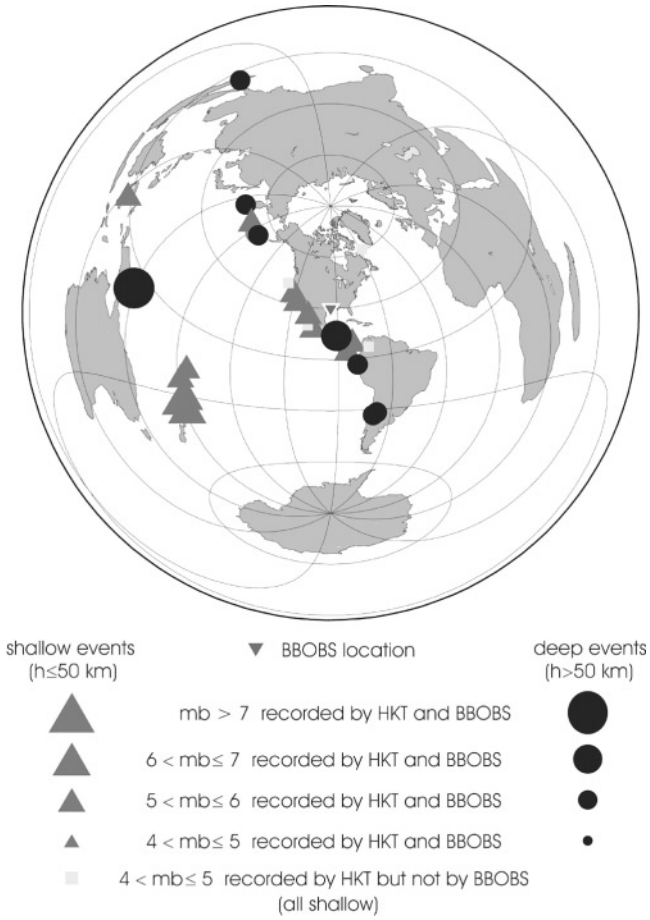

Figure 10. Map of earthquakes recorded during the Gulf of Mexico deployment. We identified 32 events (Table 1) on the BBOBS that also appeared clearly on the HKT records. In addition, we were able to identify five small events on the HKT records that were not apparent in the BBOBS data.

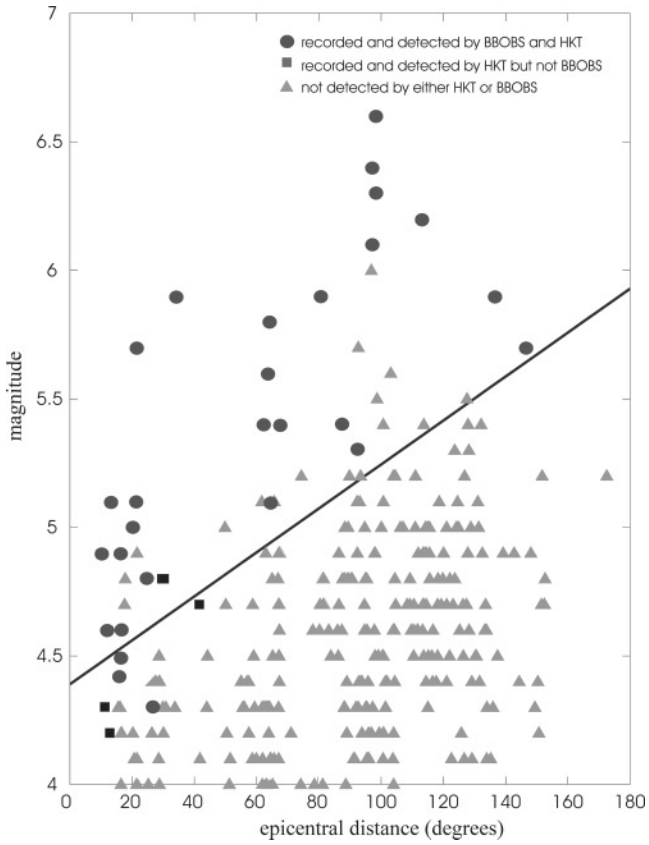

Figure 11. Magnitude versus distance plot for events that occurred worldwide during the deployment, from the National Earthquake Information Center catalog. Circles indicate events recorded by both the BBOBS in the Gulf of Mexico and the permanent GSN station HKT. Squares indicate events that could be identified in HKT data but not BBOBS data; triangles indicate events that could not be identified on either seismograph. The straight line was drawn to generally separate identified from unidentified events and thus represents a rough "detection limit" for the BBOBS at its Gulf of Mexico deployment site.

16b. A more distant and slightly smaller event from Papua New Guinea (Fig. 16c) shows relatively larger surface waves than body waves, compared with all three Kermadec Islands events, although the time separation between *SKS, SKKS*, and *S* is increased due to the greater epicentral distance. Well-dispersed surface wave trains were recorded for the Kermadec Islands and Papua New Guinea events.

A moderately deep event in Indonesia at an epicentral distance of 146.4° from the BBOBS produces a clear *PKPdf* phase, which traveled through the Earth's inner core (Fig. 17). Again, relatively more energy of this compressional phase appears on the BBOBS horizontal components when deployed on the seafloor than appears on the HKT horizontals, although some energy is clearly there as well (as indicated by the higher frequency content). A fairly small *PP* phase may be identified at HKT, but not on the BBOBS. The converse case arises for an event in Argentina, in which *P* arrivals appear prominently on both HKT and BBOBS vertical records, but it is followed by a large-amplitude *pP* phase on the BBOBS that is nearly invisible on the HKT records (Fig. 18). Closer events that occurred offshore Ecuador on 3 August 1999 ($\Delta = 33.9°$, Fig. 19) and Nicaragua ($\Delta = 16.5°$, Fig. 20) show clear *P* and *pP* arrivals but small-amplitude *S* arrivals. Figure 21 illustrates an additional type of data available only in the oceans: a waterborne *T* phase apparently generated above the 135-km-deep focus of an event in Chiapas, Mexico.

Shear Waves Recorded by the BBOBS on the Seafloor

Due to the soft sediments that cover most of the seafloor and the difficulty in installing seismographs securely in or beneath the sediments, coupling between the solid Earth and the seismograph is often suspect. Poor coupling, combined

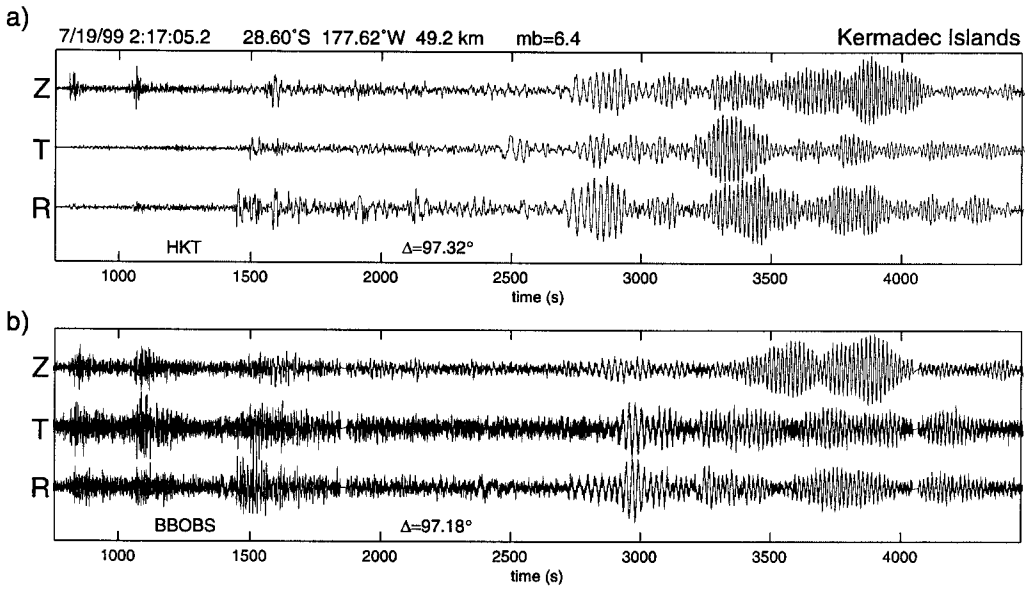

Figure 12. Seismograms from HKT (top) and BBOBS (bottom) of an earthquake on 19 July 1999 in the Kermadec Islands region (Table 1) illustrate the differences in high-frequency noise between the HKT site and the BBOBS deployed on the Gulf of Mexico seafloor. A five-pole butterworth bandpass filter with corner frequencies at 0.01 and 5 Hz has been applied, and seismograms have been trace normalized to facilitate comparison.

with exposure to bottom currents and acoustic noise in the oceans, has the potential to degrade recordings of shear waves more severely than recordings of compressional waves. However, our Gulf of Mexico deployment clearly shows that useful shear waves can be recorded by an OBS that is equipped with a broadband sensor, although degradation of the signal-to-noise ratio compared with recordings on land is often more severe than for compressional waves. Figure 22a–c shows expanded versions of the Kermadec Islands recordings for the time interval around the *S* arrival in which records were bandpass filtered with corner frequencies at 0.01 and 1 Hz. These are all shallow events, so source-side reverberations complicate phase identification. However, in most cases the direct *S* wave is clear because it appears on both the radial and transverse components. *SKS* is the first arrival in this group of phases and is polarized in the radial direction. Further identifications were made via raytracing through the iasp91 velocity model and are open to question, but the most important point is that there is a wealth of arrivals available for modeling. A combination of waveform modeling and polarization analysis could be used to sort out additional arrivals.

Not all events will produce useful shear arrivals, of course. Orientation of the focal mechanism with respect to the BBOBS, size of the earthquake, and epicentral distance dictate the amplitude of energy available to be recorded, independently of the seismograph's sensitivity and placement. The 6 August 1999 event in the Kuril Islands produces a small shear wave, even though it precedes *SKS* and *SKKS* at this distance (Fig. 23a). In contrast, the 1 August 1999 Andreanof Islands event produces a clear and prominent shear wave that is uncomplicated by other arrivals (Fig. 23b).

Discussion

The broadband seismograph and deployment strategy described here have attractive features as well as drawbacks. Attractive features include the low cost of both the instrument and of field operations involving the instrument. Drawbacks include data quality that is inferior to that of land seismographs and can be expected to be inferior to permanent stations installed in seafloor boreholes. Whether the data quality will generally be significantly inferior to broadband seismographs buried in shallow sediments is an open question. Regardless, there are important regions in which sediments are sparse or nonexistent, such as midocean ridges. Advantages and drawbacks are summarized below.

Advantages of our BBOBS strategy:

- Low cost: Parts and materials cost less than $15,000 per instrument.
- Ease of deployment/retrieval: The BBOBS does not require any specialized equipment to deploy or recover, so small, inexpensive vessels may be used.
- Small and light: At 43 cm in diameter and 35 kg (without its anchor) the BBOBS is easy and inexpensive to ship around the world, easy to handle, and does not require much deck space aboard a ship. This allows a small vessel

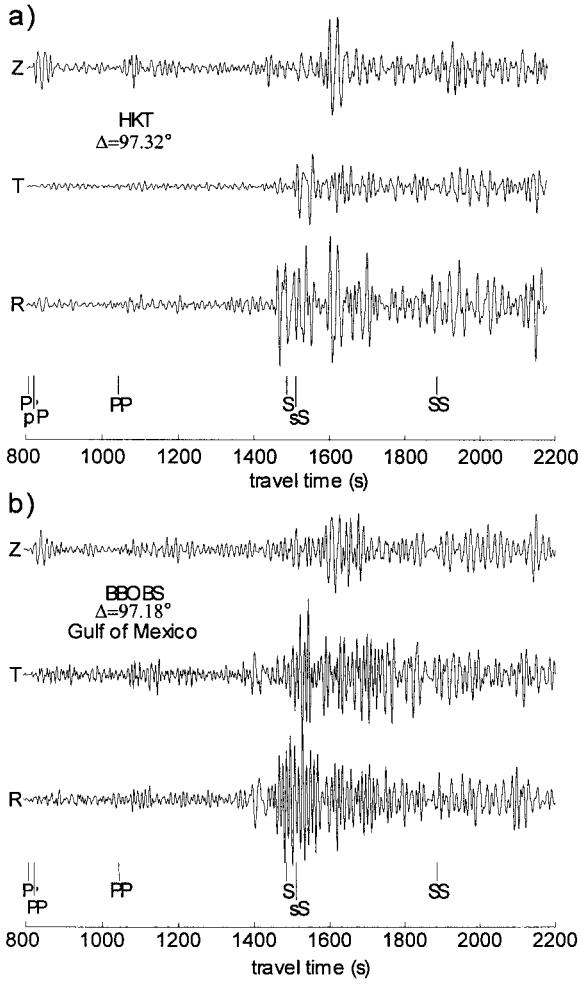

Figure 13. Comparison of body waves recorded by (a) HKT and (b) BBOBS for the 19 July 1999 Kermadec Islands event. A five-pole butterworth bandpass filter with corner frequencies at 0.01 and 0.5 Hz has been applied.

to be used and also offers a relatively small cross section to bottom currents, which can be a major source of noise in the frequency band of interest to seismologists.

- Highly reliable: The UTIG OBS has been operated since 1978 using the same deployment strategy and since 1990 with the same design. Aside from one experiment that used a different anchor design and lost 13 OBSs, over 400 drops have been conducted with the current design with the loss of only 3 instruments.
- More instruments: By keeping costs down, a fixed budget will purchase more instruments, so deployments related to a single experiment could be more densely instrumented or a broader area could be studied, or more than one experiment could be conducted simultaneously. Given the long deployment durations anticipated, a larger instrument pool would clearly be an advantage.

Potential uses of a broadband OBS, in additional to recording earthquakes at teleseismic and regional distances for investigations of deep Earth structure and earthquake source processes, include site characterization to provide design criteria for seafloor engineering projects, such as drilling and production platforms and pipelines (Huerta-Lopez *et al.*, 2002); investigations of geohazards, such as landslides, salt slumping events, and so on; and monitoring local seismicity in the ocean basins. Data from OBSs that use the same "drop" deployment strategy but seismometers with narrower passbands limited to higher frequencies have been used for applications associated with the MELT experiment on the East Pacific Rise, including an investigation of microearthquake activity (Shen *et al.*, 1997), mantle body-wave tomography (Toomey *et al.*, 1998), waveform inversion for upper mantle structure (Webb and Forsyth, 1998), shear-wave splitting measurements to constrain upper-mantle anisotropy (Wolfe and Solomon, 1998), receiver function stacking to image upper mantle discontinuities (Shen *et al.*, 1998), and measurements of Rayleigh-wave phase velocity curves to model shear velocities and anisotropy in the crust and upper mantle (Forsyth *et al.*, 1998b). These studies proved to be feasible with "drop" deployments and narrowband seismometers, but all would benefit from instruments with wider passbands and longer deployment capabilities.

Disadvantages:

- Noise levels: Noise levels can be decreased by burying the seismometer. However, burying the seismometer entails a much more costly, intricate, logistically demanding and time-intensive deployment strategy that involves relatively rare and specialized equipment. Our noise characterization results indicate that site amplification effects are largely confined to frequencies above 1 Hz. However, the band of lowest background noise in the ocean basins reaches a minimum in the band 0.03–0.1 Hz (the noise notch). Since moderate- and large-sized earthquakes generally contain a great deal of energy in this range, seismologists will probably focus there. Travel-time picks can be made at higher frequencies if greater precision is desired. While it may be appealing to lower noise levels, particularly at frequencies above 1 Hz, by burying the seismometer, the much greater cost of burial must be weighed against the improvement in data quality. However, the side-by-side test at HKT between the STS-1 and PMD 2123 indicate that the PMD's intrinsic noise in the 0.03–0.1 Hz band is higher than desirable.
- Seismometer. Despite its positive qualities for OBS applications, the PMD 2123 seismometer still has some unexplained spiking problems and its intrinsic noise levels were higher than expected above 1 Hz. However, ambient noise levels at the seafloor appear to be higher than those on continents for frequencies above 1 Hz. Using the "best" seismometer possible is often not warranted.
- Data gaps. The frequency of data gaps depends on the size

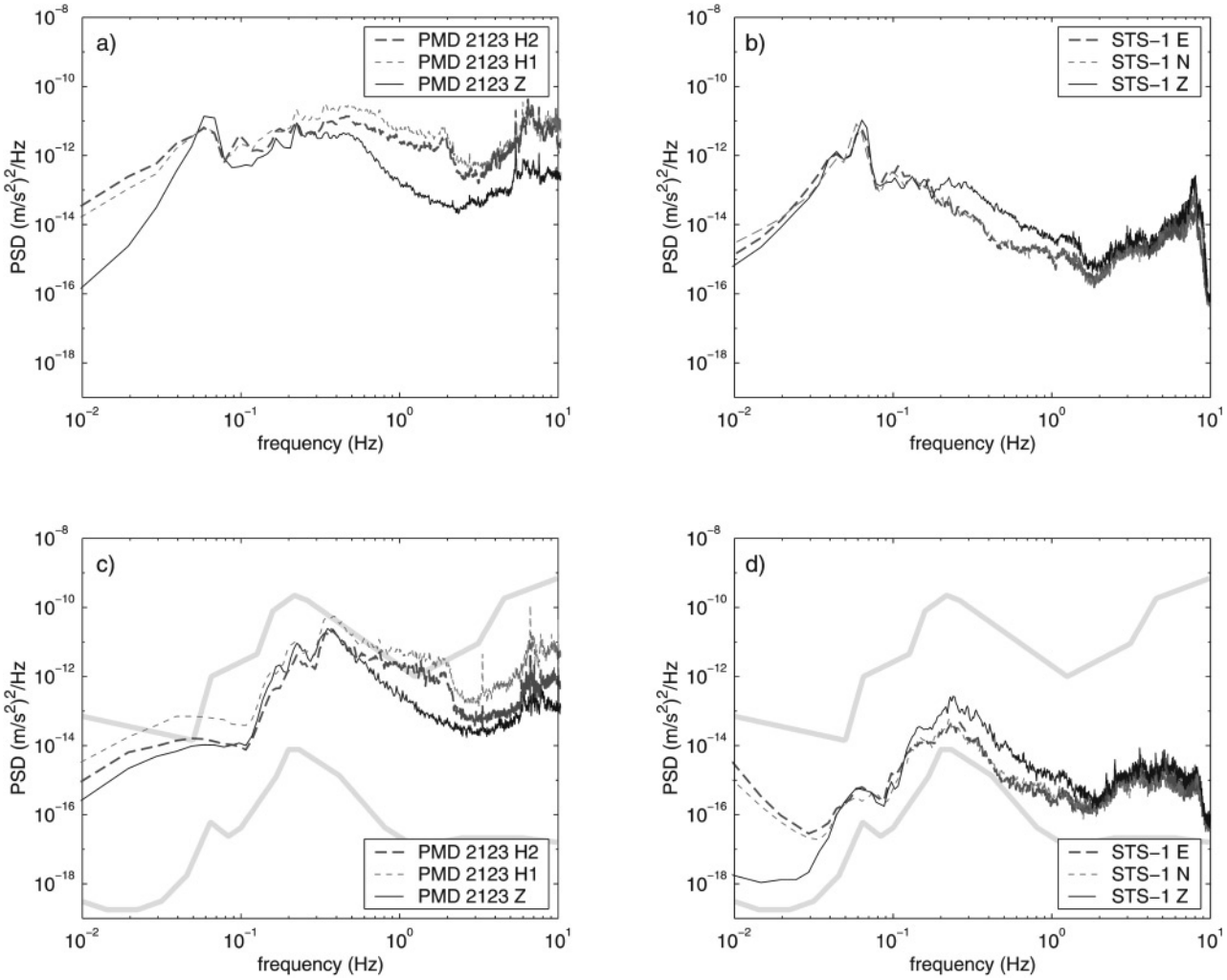

Figure 14. PSD estimates for the 19 July 1999 Kermadec Islands recordings made by (a) the BBOBS in the Gulf of Mexico and (b) station HKT, along with PSDs of the 36 min of background noise preceding the first arrivals from the earthquake at (c) the BBOBS and (d) HKT. Compared to HKT, and to the BBOBS noise recorded at Hockley shown in Figure 5, the noise recorded in the Gulf of Mexico is higher in amplitude across the entire frequency band, but the signal-to-noise ratio in the band of peak teleseismic power is still significant.

of the memory buffer. A 96-MB flash memory card (which is included in a new prototype currently being tested) will require writing to disk once every 38 hr when sampling three channels at 40 samples/sec, or once every 3 days at 20 samples/sec. As available flash memory increases in size, data gaps will become less frequent. Currently, 90% of the data gap is used for disk spin up and spin down; this is fixed overhead that does not scale with the size of the data block to be dumped. At current data transfer rates, about 2.4 min of every 38 hr would be required to write data to disk and thus would produce a data gap of less than 2.5 min each 1.5 days (when recording at 40 samples/sec). While this strategy risks missing part of an earthquake, we believe the risk is acceptably small. As disk transfer rates improve, the length of each data gap will decrease. When sampling at 20 samples/sec, the BBOBS would fail to record less than 2.4 min of every 3 days, or 0.056% of the deployment.

To eliminate data gaps entirely the seismometer would have to be deployed outside the sphere that houses the disk drive and other electronics. This would increase the size of the BBOBS overall, add to construction and deployment costs, most likely make the instrument less rugged and reliable, and complicate deployment logistics. We regard the data gaps to be acceptable trade-offs for avoiding these complications. The main advantage of external seismometer deployment would be the ability to emplace the seismometer

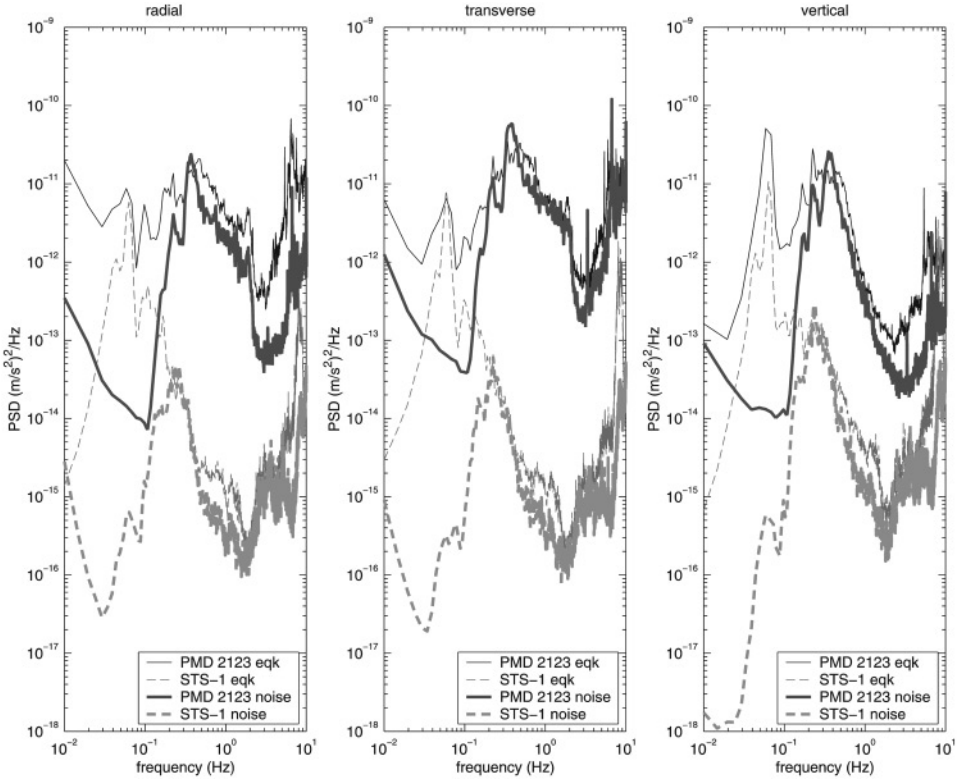

Figure 15. PSDs for background noise recorded by the BBOBS in the Gulf of Mexico (bold solid lines) compared to noise recorded by HKT on land (thick dashed lines) and for the earthquake signals shown in Figure 11. Despite the high background noise levels on the BBOBS, compared to typical levels on land, energy peaks for teleseismic events such as this one often nearly coincide with local minima in background noise power, providing impressive signal-to-noise ratios in the most important frequency band for teleseismic and far regional studies.

in or below the sediment layer to potentially improve coupling and/or reduce background noise.

Future Plans

We are in the process of upgrading the BBOBS's electronics package to an entirely new design, which will significantly reduce its power requirements and lengthen data records. The new design, currently being tested, features a 22-bit ADC with 5 V peak to peak and the same antialias filter employed currently. The dynamic range relative to electronic noise of this ADC is -116 dB when recording four channels at 40 samples/sec. The flash memory data buffer has been expanded to 96 MB, which minimizes the effects of housing the seismometer inside the glass sphere with the disk drive, as discussed earlier. The new-generation BBOBS, including the PMD 2123 seismometer and electronics package, consumes less than 250 mW when recording the three seismometer channels alone and less than 300 mW when also recording the hydrophone, due to the power requirements of the hydrophone preamplifier. Disk capacity no longer constrains deployment duration; the BBOBS currently being tested is outfitted with a 10-GB enhanced integrated drive electronics (EIDE) disk drive but will accommodate EIDE drives of even greater capacity.

Conclusions

The achievements of earthquake seismologists in determining Earth structure from core to crust are remarkable, especially since they were accomplished with a set of seismographic stations that are largely confined to the continents. While some stations are located on islands in the ocean basins, they are few in number and nowhere do they achieve the density of sampling that is routinely achieved on land. There are at least three consequences of uneven and incomplete global coverage by seismographic stations. First, since the most commonly used sources for seismic imaging of the deep Earth (earthquakes) are beyond our control, many significant features are only partly imaged, or perhaps not imaged at all. Our best hope for reliable, comprehensive imaging is to obtain dense coverage of the Earth with seismic instrumentation and to design experiments carefully, so that we make the most efficient use of available seismicity (Wysession, 1996). To execute such experiments we need seismic instrumentation with the versatility and flexibility to be de-

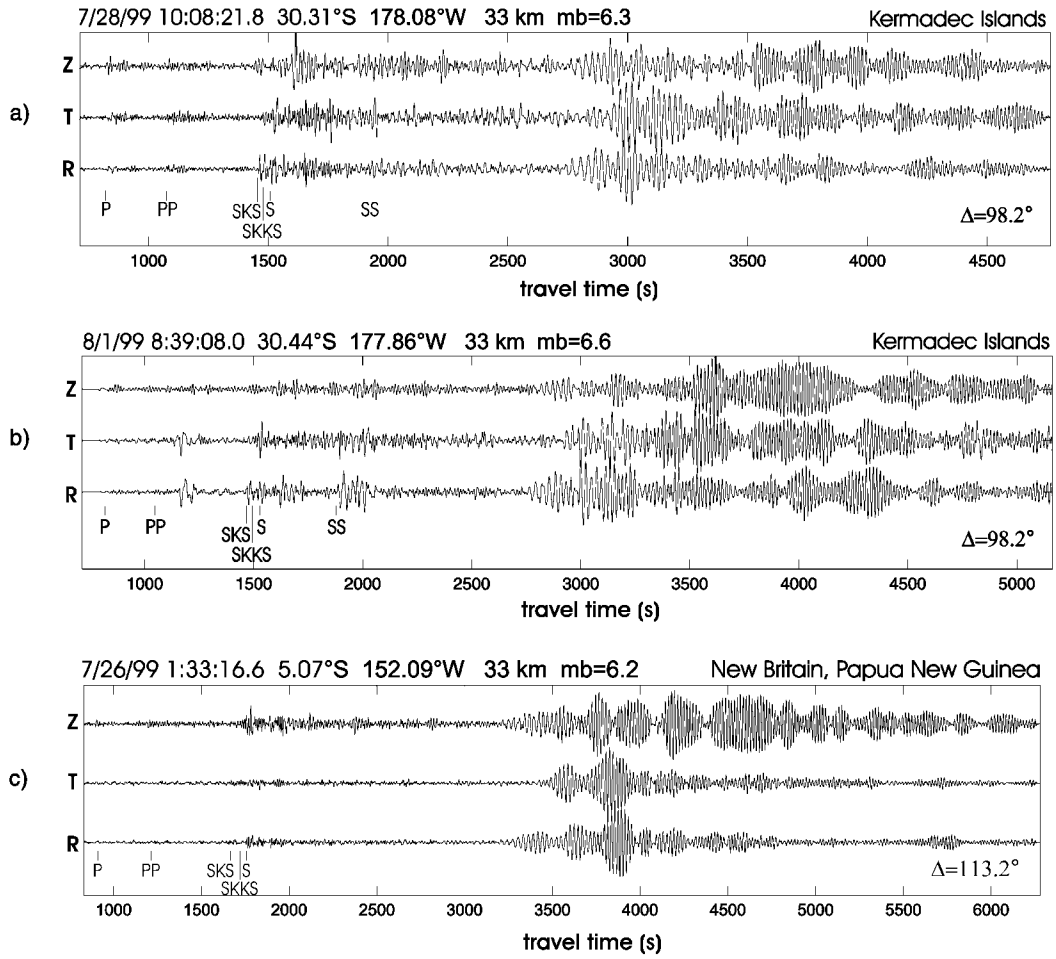

Figure 16. (a) An event in the Kermadec Islands recorded by the BBOBS on the Gulf of Mexico seafloor at an epicentral distance of 98.2°. A five-pole Butterworth bandpass filter with corner frequencies at 0.01 and 0.1 Hz has been applied. (b) An event in the Kermadec Islands recorded by the BBOBS on the Gulf of Mexico seafloor at an epicentral distance of 98.2°. A five-pole Butterworth bandpass filter with corner frequencies at 0.01 and 0.1 Hz has been applied. The large arrival appearing on the horizontal components at approximately 1150 sec is apparently unrelated to the Kermadec Islands earthquake. (c) An event in the New Britain Region of Papua New Guinea recorded by the BBOBS on the Gulf of Mexico seafloor at an epicentral distance of 113.2°. A five-pole butterworth bandpass filter with corner frequencies at 0.01 and 0.1 Hz has been applied.

ployed where and when scientific priorities demand and to be able to stay in service as long as science plans require. Furthermore, in order to make the best use of the opportunities Earth allows us, seismic instrumentation must be capable of rapid deployment and retrieval. Earthquakes tend to occur in swarms. A large event is commonly followed by a series of aftershocks, whose characteristics reveal a great deal about local tectonics. Second, our view of the deep Earth is unnecessarily obstructed when seen from the vantage point of continents. Continental crust is much thicker, more complex, and more heterogeneous than oceanic crust, yet it is the filter through which we generally view the deeper Earth. Third, the continental portion of the Earth, from which we have obtained previous insights, is not representative of the entire Earth. We know that our understanding is therefore biased, but we do not know the precise nature of differences between continents and oceans or the depths to which these differences extend. Until studies have been performed in the ocean basins that are comparable to studies performed on continents, we will not understand the nature or magnitude of our current bias.

In order to advance fundamental earth science research in the next several decades, instrumentation is needed that will allow roving seismological studies in the world's oceans. There are important roles for both fixed and portable stations in oceanic as well as continental regimes. Fixed stations typically offer higher quality data, since limitations on instrument size, power consumption, and cost are typically

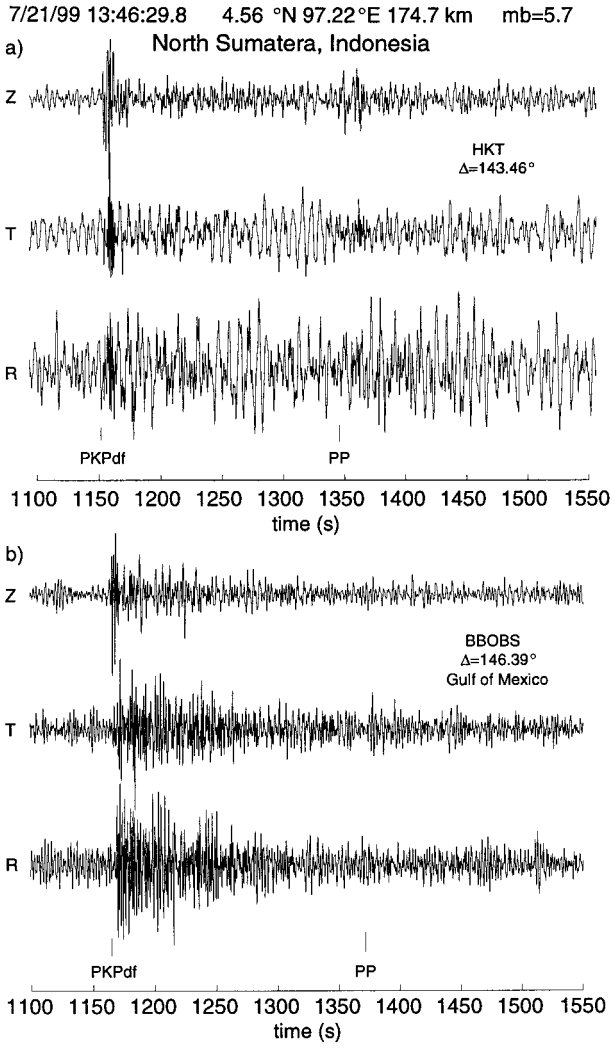

Figure 17. An event in Northern Sumatera, Indonesia, shows clear *PKPdf* arrivals, which travel through the Earth's inner core, both at (a) HKT and (b) the BBOBS on the Gulf of Mexico seafloor.

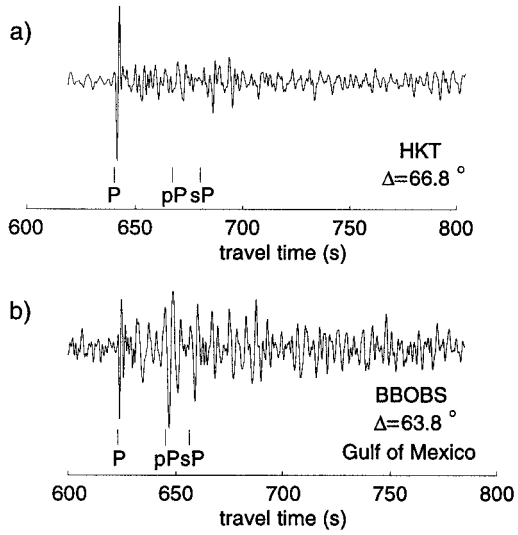

Figure 18. Vertical-component records from (a) HKT and (b) the BBOBS of an intermediate-depth, m_b = 5.4 event in the San Juan province of Argentina. The BBOBS record shows the *pP* arrival more clearly than does the HKT record, where it is barely visible.

less strict. Portable instruments "fill in the gaps" and are more amenable to experiments, both with controlled and earthquake sources, since instruments may be rearranged as scientific priorities and goals evolve. Fixed stations on and below the seafloor are being pursued (Langseth and Spiess, 1987; Forsyth *et al.*, 1991; Montagner *et al.*, 1994; Suyehiro, 1997; Stakes *et al.*, 1998) in addition to portable instruments, but they will be expensive to install and maintain. Efforts to install permanent observatories in boreholes beneath the oceans have been boosted by the Ocean Drilling Program, which plans to coordinate the installation of seismographs in some of the boreholes it drills. Portable instruments are more likely to produce scientific advances in the near future due to their flexibility, relatively low cost, and redundancy. We believe that an instrument such as the inexpensive, small, and lightweight OBS described here can play an important role in broadband seismology in the oceans, despite the fact that its data quality may be inferior to that recorded by more expensive seismographs and more elaborate de-

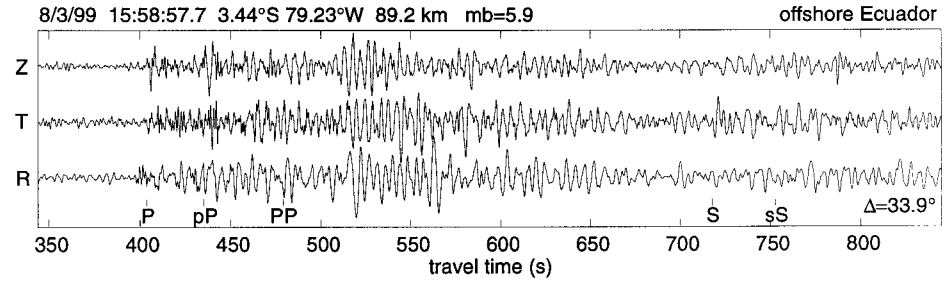

Figure 19. An intermediate-depth earthquake offshore Ecuador shows a clear *pP* phase, allowing relatively strong constraint of the focal depth.

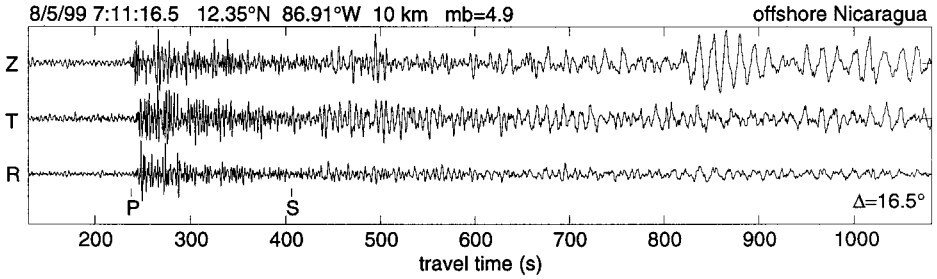

Figure 20. A very shallow event offshore Nicaragua on 5 August 1999 shows strong reverberations and scatter following the direct *P* arrival.

ployment methods. The vastness of the oceans and the dearth of broadband data collected so far ensures that the opportunity to deploy many more instruments over a greater area and/or obtain important redundancy in remote or noisy regions will compensate for the data quality.

PMD's seismometer utilizes molecular electronic transducers instead of the traditional pendulum-based design, which results in an inexpensive, small, lightweight, and rugged seismometer with low power requirements that is highly tolerant of tilt. Our BBOBS strategy focuses on developing a small, inexpensive, and highly reliable broadband seismograph that is easy to deploy and recover. These characteristics promote redundancy and dense deployments designed to target particular features and address specific scientific questions. While our BBOBS rests on top of the seafloor and is therefore subject to higher background noise levels than if the seismometer were buried in sediments, modern processing and imaging techniques, in conjunction with dense deployments, can more than compensate for the higher noise levels. Furthermore, in some areas of interest, such as midocean ridges, burial in sediments is often not an option. Materials to construct our broadband OBS cost less than $15,000; with the new electronics package under development, we anticipate that batteries and expendables for a year's deployment would cost less than $500.

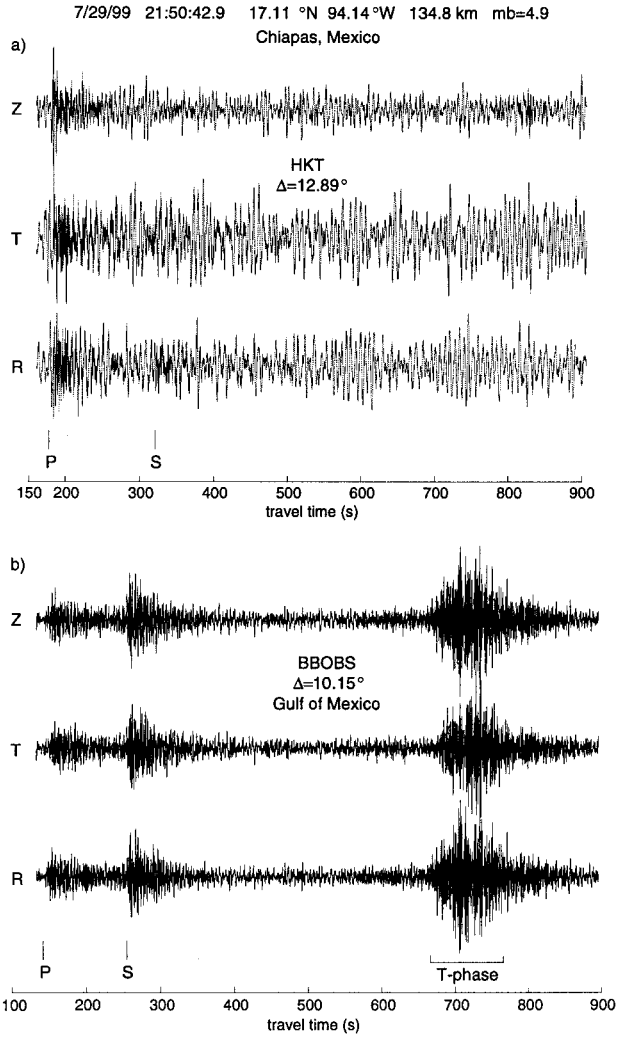

Figure 21. An event in Chiapas, Mexico, shows a strong waterborne *T* phase at the BBOBS but not at HKT, which is located roughly 100 km from the coast.

Acknowledgments

The authors thank associate editor Pujol and two anonymous referees for conducting thorough and careful reviews. Their efforts improved our original manuscript significantly. This research was supported by the Texas Higher Education Coordinating Board's Advanced Technology Program, Grant Number 003658-225-1997. UTIG Contribution Number 1586.

References

Abramovich, I. A., V. Agafonov, M. Cobern, V. Kozlov, and A. Kharlamov (1997). Improved, wide-band molecular electronic seismometer and data acquisition system, *EOS* **78,** 463.

Abramovich, I. A., M. E. Cobern, A. V. Kharlamov, and A. P. Panferov (2001). Investigation of nonlinearities in vertical sensors of MET seismometers, *Seism. Res. Lett.* **72,** 199–204.

Blackman, D. K., J. A. Orcutt, and D. W. Forsyth (1995). Recording teleseismic earthquakes using ocean-bottom seismographs at mid-ocean ridges, *Bull. Seism. Soc. Am.* **85,** 1648–1664.

Bradley, C. R., R. A. Stephen, L. M. Dorman, and J. A. Orcutt (1997). Very low frequency (0.2–10 Hz) seismoacoustic noise below the seafloor, *J. Geophys. Res.* **102,** 11,703–11,718.

Collins, J. A., F. L. Vernon, J. A. Orcutt, R. A. Stephen, K. R. Peal, F. B.

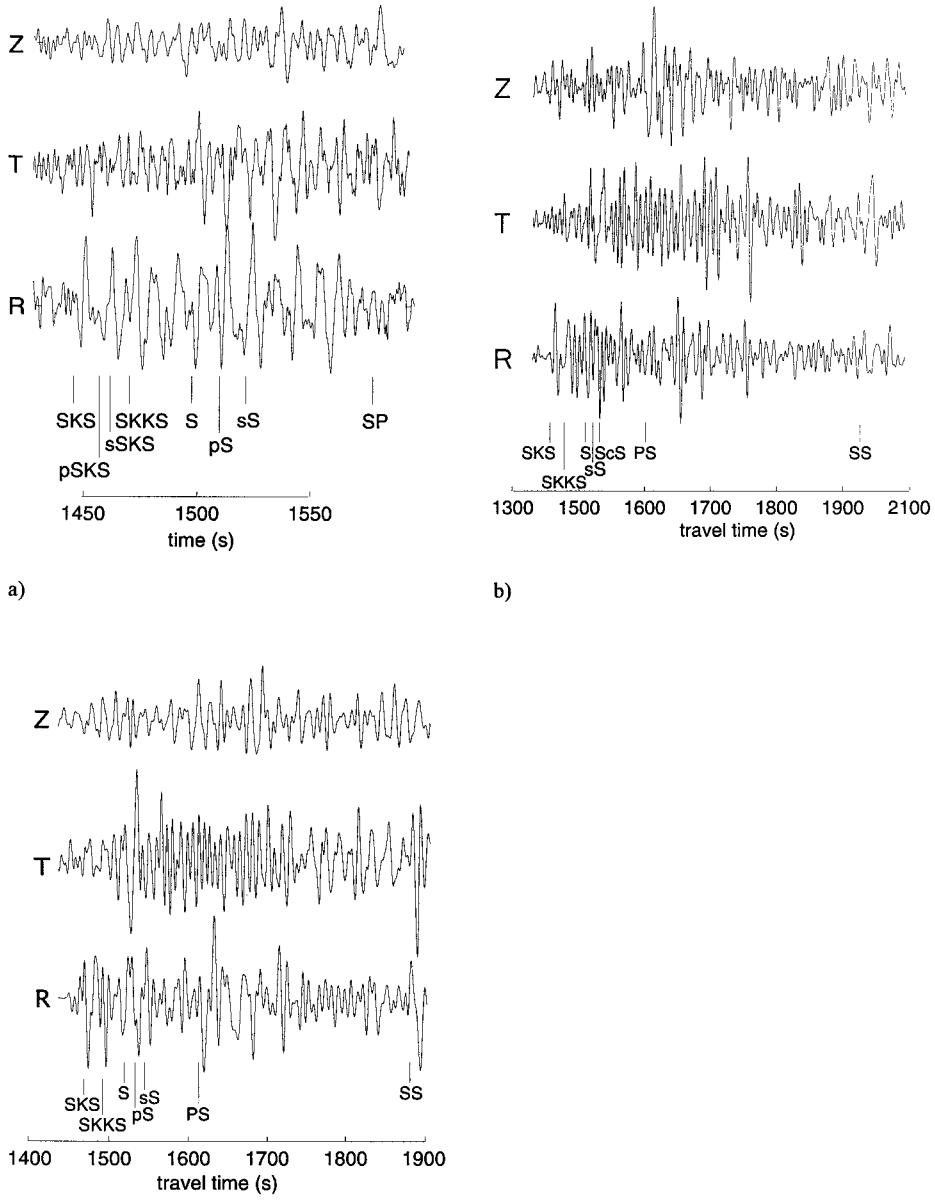

Figure 22. Shear waves recorded by the BBOBS on the Gulf of Mexico seafloor from events in the Kermadec Islands on (a) 19 July 1999, (b) 28 July 1999, and (c) 1 August 1999.

Wooding, F. N. Spiess, and J. A. Hildebrand (2001). Broadband seismology in the oceans: lessons from the ocean seismic network pilot experiment, *Geophys. Res. Lett.* **28,** 49–52.

Dozorov, T. A., and S. L. Soloviev (1991). Spectra of ocean-bottom seismic noise in the 0.01–10 Hz range, *Geophys. J. Int.* **106,** 113–121.

Duennebier, F. K. (1997). HUGO, the Hawaii Undersea Geo-Observatory, *EOS* **78,** 828.

Duennebier, F. K., and G. H. Sutton (1995). Fidelity of ocean bottom seismic observations, *Mar. Geophys. Res.* **17,** 535–555.

Forsyth, D. W., D. S. Scheirer, S. C. Webb, L. M. Dorman, J. A. Orcutt, A. J. Harding, D. K. Blackman, J. Phipps Morgan, R. S. Detrick, Y. Shen, C. J. Wolfe, J. P. Canales, D. R. Toomey, A. F. Sheehan, S. C. Solomon, and W. S. D. Wilcock (1998a). Imaging the deep seismic structure beneath a mid-ocean ridge: the MELT experiment, *Science* **280,** 1215–1218.

Forsyth, D. W., S. C. Webb, L. M. Dorman, and Y. Shen (1998b). Phase velocities of Rayleigh waves in the MELT experiment on the East Pacific Rise, *Science* **280,** 1235–1238.

Forsyth, D. W., et al. (1991). JOI/IRIS ocean seismic network, Report of the U.S. pilot experiment task force meeting, 30 pp., Joint Oceanographic Institutions, Inc., Washington, D.C.

Frohlich, C. (1982). Seismicity of the central Gulf of Mexico, *Geology* **10,** 103–106.

Huerta-Lopez, C. I., J. Pulliam, and Y. Nakamura (2002). *In situ* evaluation of shear wave velocities in seafloor sediments with a broadband ocean-bottom seismograph, *Bull. Seism. Soc. Am.* **93,** no. 1, 139–151.

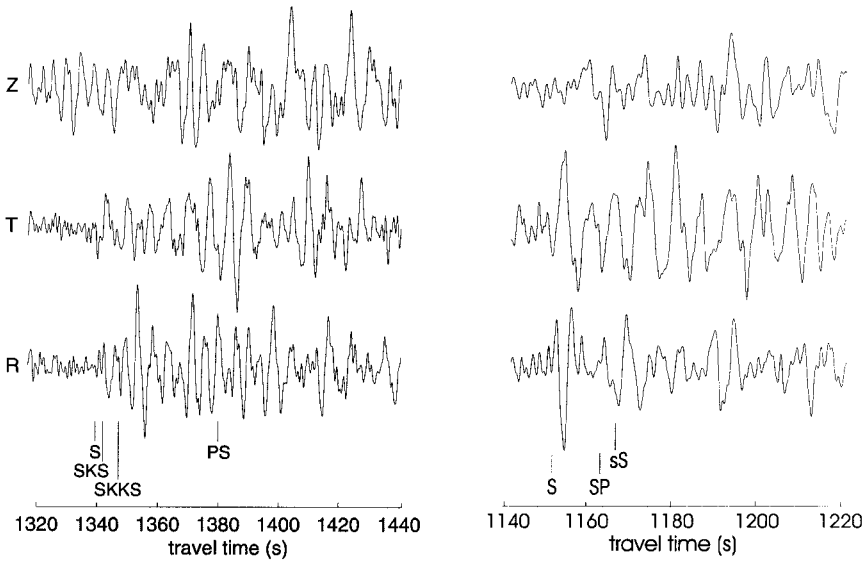

Figure 23. Shear waves recorded by the BBOBS on the Gulf of Mexico seafloor from (a) an event on 6 August 1999 in the Kuril Islands, and (b) an event in the Andreanof Islands, Alaska, on 1 August 1999.

Langseth, M. G., and F. N. Spiess (1987). Science opportunities created by wireline re-entry of deep sea boreholes, 65 pp., Joint Oceanographic Institutions, Inc., Washington, D.C.

Montagner, J.-P., J.-F. Karczewski, B. Romanowicz, S. Bouaricha, P. Lognonne, G. Roult, E. Stutzmann, J. L. Thirot, J. Brion, B. Dole, D. Fouassier, J.-C. Koenig, J. Savary, L. Floury, J. Dupond, A. Echardour, and H. Floch (1994). The French pilot experiment OFM-SISMOBS: first scientific results on noise level and event detection, *Phys. Earth Planet. Interiors* **84,** 321–336.

Nakamura, Y., P. L. Donoho, P. H. Roper, and P. M. McPherson (1987). Large-offset seismic surveying using ocean-bottom seismographs and air guns: instrumentation and field technique, *Geophysics* **52,** 1601–1611.

Peterson, J. (1993). Observations and modeling of seismic background noise, *U.S. Geol. Surv. Open-File Rept. 93-322.*

Purdy, G. M. (Editor) (1995). Broadband seismology in the oceans: towards a five-year plan, Joint Oceanographic Institutions, Inc., Washington, D.C.

Satterfield, W., and E. W. Behrens (1990). A late Quaternary canyon/channel system, northwest Gulf of Mexico continental slope, *Mar. Geol.* **92,** 51–67.

Shen, Y., D. W. Forsyth, J. Conder, and L. M. Dorman (1997). Investigation of microearthquake activity following an intraplate teleseismic swarm on the west flank of the southern East Pacific Rise, *J. Geophys. Res.* **102,** 459–475.

Shen, Y., A. F. Sheehan, K. G. Dueker, C. de Groot-Hedlin, and H. Gilbert (1998). Mantle discontinuity structure beneath the southern East Pacific Rise from P-to-S converted phases, *Science* **280,** 1232–1235.

Stakes, D. S., Romanowicz, B., J.-P. Montagner, P. Tarits, J.-F. Karczewski, S. Etchemendy, C. Dawe, D. Neuhauser, P. McGill, J. C. Koenig, J. Savary, M. Begnaud, and M. Pasyanos (1998). Seismic experiment paves way for long-term seafloor observatories, *EOS* **79,** 301, 308–309.

Suyehiro, K. (1997). Borehole observatories—global networking and 4-D monitoring, *JOIDES J.* **23,** 18–19.

Toomey, D. R., W. S. D. Wilcock, S. C. Solomon, W. C. Hammond, and J. A. Orcutt (1998). Mantle seismic structure beneath the MELT region of the East Pacific Rise from P and S wave tomography, *Science* **280,** 1224–1227.

Trehu, A. (1985). Coupling of ocean bottom seismometers to sediment: results of tests with the U.S. Geological Survey ocean bottom seismometer, *Bull. Seism. Soc. Am* **75,** 271–289.

Uhrhammer, R. (1997). Noise PSD analysis and comparison of broadband seismic sensors, in IRIS Consortium Workshop on Seismic Instrumentation, Santa Fe, NM, 10–12 November 1997.

Webb, S. C. (1998). Broadband seismology and noise under the ocean, *Rev. Geophys.* **36,** 105–142.

Webb, S. C., and D. W. Forsyth (1998). Structure of the upper mantle under the EPR from waveform inversion of regional events, *Science* **280,** 1227–1229.

Wilcock, W. S. D., S. C. Webb, and I. Th. Bjarnason (1999). The effect of local wind on seismic noise near 1 Hz at the MELT site and in Iceland, *Bull. Seism. Soc. Am.* **86,** 1543–1557.

Wolfe, C. J., and S. C. Solomon (1998). Shear-wave splitting and implications for mantle flow beneath the MELT region of the East Pacific Rise, *Science* **280,** 1230–1232.

Wysession, M. E. (1996). How well do we utilize global seismicity?, *Bull. Seism. Soc. Am.* **86,** 1207–1219.

Institute for Geophysics
University of Texas at Austin
4412 Spicewood Springs Road, Bldg. 600
Austin, Texas 78759-8500
jay@ig.utexas.edu; yosio@ig.utexas.edu; yates@ig.utexas.edu.
(J.P., Y.N., B.Y.)

Institute for Geophysics and Department of Civil Engineering
University of Texas at Austin
4412 Spicewood Springs Road, Bldg. 600
Austin, Texas 78759-8500
huerta@ig.utexas.edu
(C.H.L.)

Manuscript received 23 October 2001.